

Structural Constraints on the Exhumation of the  
Tso Moriri Dome, NW Himalaya

by

Ryan J. Clark

B.S., Geology and Geophysics (2002)

University of Wisconsin – Madison

Submitted to the Department of Earth, Atmospheric and Planetary Sciences  
in Partial Fulfillment of the Requirements for the Degree of  
Master of Science in Earth and Planetary Sciences

at the

Massachusetts Institute of Technology

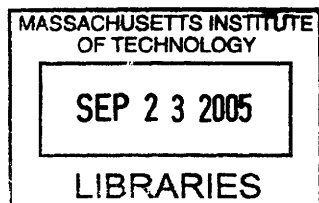
June 2005

© 2005 Massachusetts Institute of Technology  
All rights reserved

Signature of Author .....  
Department of Earth, Atmospheric and Planetary Sciences  
May 23, 2005

Certified by .....  
Kip Hodges  
Professor of Geology  
Thesis Supervisor

Accepted by .....  
Maria Zuber  
E. A. Griswold Professor of Geophysics  
Department Head



ARCHIVES

**NOTICE: THIS MATERIAL MAY BE  
PROTECTED BY COPYRIGHT LAW  
(TITLE 17 US CODE)**

## Abstract

The Tso Morari culmination in the Ladakh region of northwest India is a large (>3,000 km<sup>2</sup>) structural dome cored by coesite-bearing rocks of Indian continental crustal affinity. As one of only two localities in the Himalaya where ultrahigh-pressure rocks have been found, the culmination offers important insights into the orogenic processes responsible for exhumation of subducted continental crust. New, 1:50,000 scale geologic mapping and structural analysis in the Tso Morari area reveals evidence for five distinct deformational events. Rather than simple, one step processes envisioned by investigators in many ultrahigh-pressure terrains, exhumation of the Tso Morari culmination was a polyphase process. From >90 km to mid-crustal depths, exhumation was accommodated by a diachronous set of rooted, ductile, extensional detachments that were active ~53-40 Ma. Beginning in the Late Oligocene, continued exhumation occurred by progressive unroofing along a younger, brittle-ductile detachment. Through a rolling-hinge mechanism similar to that proposed for many metamorphic core complexes of the North American Cordillera, this unroofing led to the development of the culmination into a NW trending structural dome. More recently, N-S-striking normal faults accommodated continued upper crustal extension throughout much of the remainder of Cenozoic time, despite the culmination's setting in the Himalayan collisional orogen.



## Introduction

The presence of ultrahigh-pressure mineral assemblages in rocks of continental affinity implies the subduction of continental crust to depths of 65-90 km (Rumble et al., 2003). Understanding the mechanism (or mechanisms) by which rocks containing ultrahigh-pressure assemblages are exhumed remains one of the more intriguing problems in continental tectonics today. Many tectonic models have been proposed (e.g., Kurz and Froitzheim, 2002), but the most viable feature some mechanism capable of explaining the very rapid rates of exhumation required for the preservation of ultrahigh-pressure assemblages with relatively minor retrogression. These models often invoke tectonic denudation by normal-sense slip on deeply rooted detachments (Chemenda et al., 1996). However, in many ultrahigh-pressure terrains, the geometry and kinematics of extensional structures that might have been responsible for exhumation remain poorly constrained.

In an effort to shed additional light on the role of extensional deformation on the exhumation of subducted continental crust, we have conducted a structural study of a portion of the Tso Morari metamorphic culmination in the Ladakh region of northwest India. With an area of at least 2,250 km<sup>2</sup>, the Tso Morari culmination is the largest exposure of ultrahigh-pressure rocks in the Himalayan-Tibetan orogenic system. Previous work in the core of the culmination has demonstrated the existence of coesite-bearing assemblages that developed during the initial stages of India-Eurasia collision (Mukherjee and Sachan, 2001). From a tectonic perspective, it is noteworthy that the Tso Morari culmination is also the largest of the so-called “North Himalayan gneiss domes”, a belt of culminations that stretches along much of the length of the Himalaya between

the range crest and the Indus-Tsangpo suture (Hodges, 2000). While many models have been proposed to explain these features (e.g., Chen et al., 1990; Guillot et al., 1998; Lee et al., 2000; Beaumont et al., 2001; Murphy et al., 2002; Lee et al., 2004), most involve an important component of extensional deformation similar to that responsible for the metamorphic core complexes of the North American Cordillera (Coney and Reynolds, 1980; Armstrong, 1982). Our studies confirm the suggestion by de Sigoyer et al. (2004) that extension played an important role in the evolution of the Tso Morari culmination. However, detailed mapping of critical contact relationships has allowed us to achieve substantially better resolution of the deformational sequence responsible for the exhumation of ultrahigh-pressure rocks in the Tso Morari core. Specifically, we conclude that unroofing was accommodated by a diachronous set of rooted detachments, comparable structurally to those found in the Basin and Range Province of western North America (Wernicke, 1985; Davis et al., 1988).

## **Geological Setting of the Tso Morari culmination**

The southern margin of the Himalayan-Tibetan orogenic system is traditionally divided into a series of tectonostratigraphic units of Indian and Eurasian affinity separated by the Indus-Tsangpo suture. The northernmost exposures of Indian Plate rocks belong to the Tibetan Zone. They consist primarily of unmetamorphosed, Paleozoic-Eocene carbonate and clastic rocks of the Tibetan Sedimentary Sequence, but also include isolated metamorphic and igneous complexes of varying ages in the South Himalayan gneiss domes (Hodges, 2000). One of these is the Tso Morari culmination, which lies in the Rupshu district of Ladakh. The culmination is named for a spectacular,

high-altitude lake – Tso Morari – that occurs on the floor of a Quaternary graben in the central part of the culmination. The gneisses of the Tso Morari culmination lie within a NW-SE trending structural dome. The northwestern termination of the dome is easily accessed and plunges moderately NW (Steck et al., 1998). The southeastern termination has not been mapped because it lies in a politically sensitive border zone between India and Tibet. Known exposures of the high-grade infrastructure of the Tso Morari culmination cover an area of  $\sim 2250 \text{ km}^2$ . The infrastructure is bound to the north by rocks of the Indus-Tsangpo Suture Zone (Berthelsen, 1953) and to the south and west by sedimentary rocks of the Tibetan Zone (Garzanti et al., 1987; Gaetani and Garzanti, 1991). The area was first described by Berthelsen (1953), and has since been mapped in reconnaissance by a number of authors (Thakur, 1983; Steck et al., 1998; de Sigoyer et al., 2004). In addition, it has been the focus of several petrologic and geochronologic studies in recent years (de Sigoyer et al., 1997; Guillot et al., 1997; Girard and Bussy, 1999; Leech et al., in press).

The identification of coesite as inclusions in garnet from rocks within the Tso Morari infrastructure (Mukherjee and Sachan, 2001) sets this dome apart from the other North Himalayan gneiss domes. The presence of such ultrahigh-pressure assemblages within rocks of continental affinity implies significant subduction of continental crust during Eocene collision of India and Asia. However, the Tso Morari culmination shares many structural similarities with other North Himalayan gneiss domes (Hodges, 2000), and occupies the same orogen-scale structural setting, within the Tibetan Zone, north of the South Tibetan fault system (Burchfiel et al., 1992).

## **Tectonic Stratigraphy**

Our field study focused on the Tso Morari infrastructure, which retains lithologies and structures related to the culmination's exhumation from ultrahigh-pressure conditions. The gross geometry of the Tso Morari culmination is similar to that of the other North Himalayan gneiss domes, where the domal structure is defined by planar fabric in the infrastructure which dips gently away from the core. The infrastructure is overlain by a suprastructure composed of low-grade metasedimentary rocks, which also dip gently away from the core of the dome.

### **Rocks of the Tso Morari Infrastructure**

#### ***The Puga Gneiss Complex***

The Tso Morari dome is cored by the Puga Gneiss Complex (Fig. 1). This unit is dominated by a medium to coarse-grained, strongly mylonitic, quartzo-feldspathic augen gneiss, but also contains lenses of peraluminous granite, amphibolite, and eclogite, as well as discontinuous layers of metasedimentary schist. The complex has also been referred to as the Tso Morari Unit by de Sigoyer et al. (2004), and the Tso Morari Granite Gneiss by Steck et al. (1998). In outcrop, the orthogneiss commonly forms white to light-gray, blocky cliffs (2-5m, though in places much higher) and is generally unaltered. The orthogneiss consists of quartz + plagioclase + K-feldspar + phengite ± biotite ± tourmaline. Quartz was dynamically recrystallized, forming ribbons up to 2 cm long that are typically pinned by micaceous layers. Where quartz is not pinned, grains show serrated grain boundaries and undulatory extinction. Potassium feldspar augen, where present, range in size up to several centimeters across and are commonly symmetric.



Micas (phengite and biotite) are strongly aligned to define the unit's gneissosity. This layering is deflected around the margins of K-feldspar augen (Fig. 2a). Tourmaline occurs as cm-scale needles, randomly oriented on planes parallel to gneissosity.

The outcrop appearance and mineralogy of the orthogneiss are similar to another felsic unit within the Puga Gneiss Complex: the peraluminous Polokong La granite. This granite (not differentiated on our maps) occurs as decameter-scale lenses in the orthogneiss near the headwaters of the Puga Valley and, less commonly, in scattered lenses to the south near the lake Kiagar Tso. Only the margins of these lenses are deformed, while the cores are coarse-grained and display granitic textures. Zircons in both the Polokong La granite and the orthogneiss yield U-Pb dates of  $479 \pm 2$  Ma, which suggest that the Polokong La granite may be the undeformed protolith of the PGC (Girard and Bussy, 1999).

Characteristically phengite-rich schistose rocks are distributed throughout the Puga Gneiss Complex as discontinuous, meter-thick layers and lenses that persist for tens of meters along strike. These layers, which are too small to be differentiated on our maps, characteristically weather a deep reddish-gray. The rocks contain phengite + quartz + plagioclase  $\pm$  biotite  $\pm$  garnet  $\pm$  kyanite  $\pm$  jadeite  $\pm$  glaucophane. Retrograde assemblages are rich in chlorite, often mantling garnet, suggesting regression of both garnet and phengite. Albite is also present as a retrograde product of the breakdown of glaucophane and garnet. Contacts between orthogneiss and schist are sharp and parallel to the schistosity in the metasedimentary rocks and gneissic layering in the orthogneiss.

Among the most distinctive features of the Puga Gneiss Complex are dark brown to black, meter-scale lenses or boudins of amphibolite and eclogite. These lenses,

interpreted as metabasalts by de Sigoyer et al. (1997), lie parallel to the gneissic layering in the surrounding gneisses. The eclogites are fine to medium-grained, with the primary assemblage garnet + omphacitic clinopyroxene + phengite ± rutile ± epidote ± quartz ± glaucophane, with accessory coesite, talc, Mg-calcite, aragonite, dolomite, apatite, and (rarely) zircon. A secondary assemblage displaying breakdown of omphacite to form intergrowths of augite and albite is displayed in some samples. All samples display a retrograde, chlorite rich assemblage due to breakdown of glaucophane, garnet and phengite. Some samples, however, show no record of the ultrahigh-pressure eclogite facies event, instead containing an assemblage dominated by hornblende, plagioclase, chlorite and occasional epidote. These samples were likely heavily recrystallized under amphibolite-facies retrogression, perhaps as a result of greater volatile content relative to less retrogressed samples (Guiraud et al., 2001).

### ***Zoboshisha Unit***

Steck et al. (1998) were the first to recognize a distinct package of schistose metasedimentary rocks containing scattered lenses of amphibolite, on the margin of the Puga Gneiss Complex near Sumdho Village (Fig. 3). Through our mapping near the villages of Sumdho and Thupse (near Tso Kar; Fig. 4), we have demonstrated that these rocks comprise a distinctive and structurally higher tectonic package that is separated from the Puga Gneiss Complex by the Karla Detachment (see below). Most rocks in this unit are metaclastic, containing quartz + phengite + albite ± biotite ± garnet ± calcite ± chlorite with accessory zircon, apatite, monazite, allanite, magnetite and rutile. They are strongly deformed and display a well-developed schistosity. Especially in outcrops near

Sumdho Village, these schists are deeply weathered to a dark reddish brown color. Scattered within the schists are black, fine-grained amphibolite boudins, similar in structural style, shape and size to those mafic boudins within the Puga Gneiss Complex. However, none of these boudins display eclogite-facies mineralogy and instead contain the characteristic assemblage garnet + plagioclase + hornblende + quartz + biotite.

This unit was correlated by Steck et al. (1998) to the Phe Formation, a sequence of Precambrian to Cambrian slates, sandstones and dolomites which was first described in the Spiti Valley by Hayden (1904). Unfortunately, there are no fossils preserved in the metamorphosed sediments around the Tso Morari culmination to confirm a Precambrian/Cambrian age for these rocks, nor is there structural continuity with the Phe Formation in the Spiti Valley, making the correlation suggested by Steck et al. (1998) difficult to confirm. While the unit's structural setting and composition suggests that it is indeed part of the Indian passive margin, there are no cross-cutting or clearly intrusive relationships to constrain the unit's age. Since the true protolith for these rocks remains unclear, they are referred to here informally as the Zoboshisha Unit, after the broad ridge on which the rocks are exposed near Sumdho Village.

## **Suprastructure of the Tso Morari Dome**

### ***Taglang La Formation***

Structurally above the Zoboshisha Unit is a sequence of low-grade marble, slate, calc-schist, meta-rhyolite, calcareous sandstone and quartzite referred to as the Taglang La Formation by Thakur and Viridi (1979). In the study area, the structurally lowest member of this formation is a massive, Fe-rich, red-weathering carbonate, locally

recrystallized and weakly metamorphosed. These rocks are distinctly visible on satellite imagery as well as in the field, forming the high peaks just east of Thupse Village. Farther upsection, the formation consists predominantly of slates and calc-schists, commonly bearing tremolite and actinolite porphyroblasts. Near Nalbukar (a camping ground north of Thupse Village), the calc-schists are intercalated with a thick sequence described by Steck et al. (1998) as meta-rhyolite (Fig. 4). Thakur and Viridi (1979) described Permian conodonts from outcrops of the Taglang La Formation 20 km northwest of Tso Kar. Unfortunately, no fossils have been found in this unit within the study area. Other authors have referred to similar Permian sedimentary rocks in the Spiti Valley 60 km south of the study area as the Kuling Formation (Stutz, 1988; Colchen et al., 1994). Fuchs and Linner (1996) proposed the term “Karzok Formation” for all Permian rocks surrounding the Tso Morari dome. We have instead adopted the original Taglang La nomenclature because the unit can be traced on Landsat 7 ETM+ imagery from just west of Tso Kar to Taglang La, a high pass ~30 km to the northwest.

### ***Lamayuru Formation***

On the southern flank of the Tso Morari dome, the sequence overlying the Puga Gneiss Complex is considerably different from that on the northern margin. The lowest exposed unit, which is faulted against the Puga Gneiss Complex along the Thupse Detachment (see below), is a sequence of interbedded marls, limestones, dolomites, shales and sandstones, exposed in a normal stratigraphic order (Steck et al., 1998). A few metabasic horizons are present, containing mineral assemblages that include albite, chlorite and actinolite. This unit is mapped by Steck (2003) as part of the Lamayuru

Formation, a sequence deposited during Early Permian to Late Cretaceous time on the north Indian continental slope.

### ***Karzok Complex***

At Karzok Village, a 300m-thick complex of serpentinites, meta-basalts, meta-gabbros, and calc-schists sits structurally above the Lamayuru Formation. These strongly deformed mafic rocks form a thin tectonic slice representing an intraoceanic arc ophiolite (Berthelsen, 1953; Maheo et al., 2000) of probable Mesozoic age (Steck et al., 1998). The meta-basalts contain albite, epidote, chlorite, actinolite and hornblende.

### ***Phe Formation***

South of the Karzok Complex and structurally above it rests a sequence of slates, sandstones and rare matrix-supported pebble conglomerates. North of the Mata Range, this unit outcrops poorly, forming only sparse, deeply weathered ridges along the shore of Tso Morari. Contact relationships with the Ordovician Rupshu Granite (see below) suggest that this unit is of Cambrian to Precambrian age.

### ***Rupshu Granite***

The Rupshu granite is exposed as an elongate pluton along the crest of the Mata Range, south of Karzok Village, about 35 km long and 5 km wide at its widest point (Fig. 1). It contains the assemblage quartz + plagioclase + biotite + K-feldspar ± titanite ± phengite ± garnet ± secondary epidote, with accessory zircon, allanite, apatite and rutile. While the compositions of the Rupshu Granite and the Puga Gneiss Complex are similar,

magmatic texture is well preserved in parts of the Rupshu Granite, while the majority of the Puga Gneiss Complex is strongly deformed. The pluton is in intrusive contact with the Phe Formation. The margin is marked by a thin rim of aplite while the adjacent Phe Formation has been subjected to local contact metamorphism (Girard and Bussy, 1999). Zircon U-Pb data for the Rupshu Granite suggest a crystallization age of  $483 \pm 1$  Ma, and the pluton is interpreted to represent a phase of magmatism distinct from that of the Puga Gneiss Complex (Girard and Bussy, 1999).

### ***Sumdho Complex and the Indus-Tsangpo Suture Zone***

The Sumdho Complex consists of an intensely deformed sequence of greenschist-amphibolite facies slates, carbonate rocks, calc-schists and metavolcanics. This unit forms large cliffs immediately NE of the Puga Gneiss Complex (Fig. 5) and continuing up the Karla Valley towards Mahe. Thick, conspicuous blocks of white limestone located within the cores of large-scale isoclinal folds were recognized and termed “exotic” by Berthelsen (1953). Previous studies have referred to this unit as the Zildat Ophiolitic Mélange (Thakur and Viridi, 1979) or the Sumdho Complex (Steck et al., 1998), while de Sigoyer et al. (2004) subdivide the unit into the Ribil and Drakkarpo Units. Based on geochemical similarities between these metavolcanic rocks and ocean island basalts (de Sigoyer, 1998) suggests that these units represent a remnant of a seamount accreted to the north Indian margin.

To the northeast, the Sumdho Complex is thrust over gabbros, sheeted dikes and pillow basalts of the Nidar Ophiolite. Southeast of the study area, the Nidar ophiolite displays a complete ophiolitic section, from ultramafic dunites and harzburgites through

gabbros and pillow lavas interbedded with chert horizons (Sachan, 2001). In the Karla Valley between Sumdho Village and Mahe, however, the sequence is disrupted and ultramafic rocks are absent. Immediately beneath the Sumdho Complex lies a gabbroic body locally altered to serpentinite. Moving north, a sequence of sheeted dikes is overlain by approximately 1 km of well-preserved pillow lavas. Geochemical evidence suggests an intraoceanic arc setting for the formation of this unit (Thakur and Bhat, 1983; Maheo et al., 2000; Sachan, 2001).

The Nidar Ophiolite is, in turn, thrust over the Indus Mollase, marking the transition from rocks of Tethyan affinity to those of Asian affinity. This unit was formed during the closure of the Tethys ocean, and records changing sedimentation from marine to continental facies. The base of the unit is composed of detritus shed from the Ladakh batholith in a fore-arc basin, interbedded with limestones, slates and siltstones. Overlying these marine sediments are the terrestrial, alluvial fan and lacustrine deposits of early Eocene age (Garzanti and Van Haver, 1988). These sediments include sandstones, megacrystic conglomerates and stretched clast conglomerates of the Hemis Conglomerate and Nulra Formation, which record the final collision of Ladakh with India.

## **Metamorphic History**

Initial studies of the Tso Moriri culmination recognized that many of the mafic boudins in the Puga Gneiss Complex contain relict eclogite assemblages (Berthelsen, 1953; Thakur and Viridi, 1979). Earlier workers also noted the northward increase in the degree of metamorphism from unmetamorphosed sedimentary rocks near the village of Chikkim in the Spiti Valley through amphibolite and eclogite facies rocks in the Tso

Morari culmination. Later metamorphic studies, including element-partitioning thermobarometry, were aimed at placing quantitative constraints on the metamorphism of both the Tso Morari infrastructure and suprastructure. However, some critical tectonostratigraphic elements were not sampled in the course of earlier studies and the complete metamorphic history of the infrastructure is not yet known.

### ***Pressure-Temperature Evolution of the Puga Gneiss Complex***

Of all tectonostratigraphic units at Tso Morari, the most comprehensive pressure-temperature (PT) paths have been established for rocks of the Puga Gneiss Complex (Fig. 6; Guillot et al., 1995; de Sigoyer et al., 1997; Guillot et al., 1997; Sachan et al., 1999; Mukherjee and Sachan, 2001; Mukherjee et al., 2003). The entrapment of coesite inclusions near the rims of garnets in eclogite pods requires a minimum pressure for peak ultrahigh-pressure metamorphism ( $M_1$ ) of 2.2 GPa. Based on various lines of evidence, Mukherjee et al. (2003) suggested peak  $M_1$  temperatures of  $>750^\circ\text{C}$  and peak pressures in excess of 3.9 GPa. These pressure estimates are based on the geobarometer of Massonne and Schreyer (1989) for silica content in phengite, and have yet to be corroborated by any other geobarometers. Such high pressure estimates would place the Puga Gneiss Complex within the diamond stability field, though no micro-diamonds have yet been reported.

The age of the  $M_1$  event remains enigmatic. de Sigoyer et al. (2000) reported low-precision Sm-Nd and Lu-Hf internal isochrons for  $M_1$  eclogite assemblages that suggest crystallization at about 55 Ma. Leech et al. (in press) obtained U-Pb SHRIMP dates of  $48 \pm 1$  Ma ( $2\sigma$ ) for metamorphic rims on zircon from a Puga Gneiss Complex orthogneiss, and they interpreted this as the age of  $M_1$  metamorphism. However, the polymetamorphic



history of the Puga Gneiss Complex (described below) suggests that alternative interpretations are possible; the metamorphic rims dated by Leech et al. (in press) cannot be unequivocally linked to ultrahigh-pressure metamorphism because the orthogneiss does not contain ultrahigh-pressure assemblages. Efforts are underway at MIT to date accessory zircons in the coesite-bearing eclogites in order to better constrain the age of  $M_1$ .

A second phase of metamorphism ( $M_2$ ) is defined by the reaction of garnet + jadeite in metapelitic units of the Puga Gneiss Complex to form glaucophane and paragonite, suggesting decompression of the Tso Moriri core with little cooling (Guillot et al., 1997). In the mafic eclogites, a second generation of glaucophane growth and the transformation of omphacite to symplectitic intergrowths of sodic augite and albite signifies partial re-equilibration at blueschist facies (de Sigoyer et al., 1997). Conditions of  $M_2$  metamorphism range from about 540-600° C, with pressure decreasing to about 1.0-1.2 GPa (de Sigoyer et al., 1997; Guillot et al., 1997). The age of  $M_2$  is also poorly constrained; de Sigoyer et al. (2000) report internal Sm-Nd and Rb-Sr isochrons for  $M_2$  assemblages that imply dates of  $47 \pm 11$  and  $45 \pm 4$  Ma, respectively.

Many metapelitic and metabasic samples from the Puga Gneiss Complex show evidence for retrogression at greenschist facies ( $M_3$ ). Although the PT conditions of this event are not constrained thermobarometrically, de Sigoyer et al. (2000) inferred  $M_3$  pressures of ~0.3-0.5 GPa and temperatures of ~200-350°C. Recrystallized muscovite and biotite from a Puga Gneiss Complex metapelitic sample have yielded  $^{40}\text{Ar}/^{39}\text{Ar}$  plateau dates of ~30 Ma, leading de Sigoyer et al. (2000) to assign this age to the  $M_3$  event.

### ***Pressure-Temperature Evolution of the Zoboshisha Unit***

Unfortunately, there have been no quantitative PT studies as yet on the metasedimentary rocks of the Zoboshisha Unit, but petrographic and semiquantitative studies of metamorphic chemical chemistry strongly suggest a metamorphic history distinctive from that of the underlying Puga Gneiss Complex. The lack of eclogite facies mineral assemblages in mafic boudins within the Zoboshisha Unit strongly suggests that the Zoboshisha Unit did not experience  $M_1$  metamorphic conditions. This conclusion is supported by the absence in the metasedimentary rocks of glaucophane or jadeite – both nearly ubiquitous in metapelitic rocks of the Puga Gneiss Complex (Guillot et al., 1997). However, parallelism of the dominant gneissic fabric in the Puga Gneiss Complex and the dominant schistosity in the Zoboshisha Unit, and the fact that  $M_2$  assemblages define the gneissic fabric in the Puga Gneiss Complex (de Sigoyer et al., 2004), suggest that the Zoboshisha and Puga Gneiss units shared a common metamorphic history from  $M_2$  onward. The mineral assemblages present in the metapelitic rocks of the Zoboshisha Unit are consistent with this interpretation (Wei and Powell, 2004), but provide no direct confirmation of it because of the low thermodynamic variance of typical mineral assemblages. Near Sumdho Village, mafic boudins within the Zoboshisha Unit do not display eclogite facies mineralogy. Instead, these rocks contain a garnet-amphibolite assemblage which again suggests that these rocks experienced peak pressures lower than those of the Puga Gneiss Complex. Many samples from the Zoboshisha Unit, particularly those collected near faults that bound the infrastructure, contain retrograde (greenschist facies) assemblages that we interpret as having formed during  $M_3$ .

### ***Suprastructure Metamorphism***

Rocks of the Tso Morari suprastructure record only M<sub>3</sub> metamorphism, and in places are almost completely unmetamorphosed. In the Taglang La Formation, carbonates are recrystallized into sugary-textured marbles, whereas calc-schist horizons are chlorite-rich and occasionally contain abundant tremolite and actinolite porphyroblasts. In the Sumdho Complex and overlying units of the Indus-Tsangpo Suture Zone, similar conditions are evidenced by an abundance of chlorite-grade minerals.

### **Structural History of the Infrastructure**

In order to inform the development of structural models for ultrahigh-pressure exhumation at Tso Morari, we combined detailed (1:50,000) structural mapping of critical areas with reconnaissance geologic photo interpretation of Landsat 7 ETM+ satellite imagery. The latter effort proved extremely useful because major lithostratigraphic units were easily traced in multispectral images, and we were able to link important structures across inaccessible terrain and to extrapolate these structures beyond the areas studied in detail.

de Sigoyer et al. (2004) assigned the deformational fabrics of the Puga Gneiss Complex to three phases based on cross-cutting relationships (While they used the traditional nomenclature of D<sub>1</sub>, D<sub>2</sub>, and D<sub>3</sub> when referring to these events, we will call them D<sub>A</sub>, D<sub>B</sub>, and D<sub>C</sub> to avoid confusion with our nomenclature). D<sub>A</sub> included rare steep, tight-to-isoclinal folds found in the core of the dome. The predominant ductile fabrics in the complex were assigned to D<sub>B</sub>, whereas fabrics thought to be related to the

development of late bounding faults separating the infrastructure and suprastructure were assigned to  $D_C$ . We found this tripartite subdivision of fabrics inadequate to describe the structure in the Puga Gneiss Complex, and we have instead assigned them to five deformational phases,  $D_1$  through  $D_5$ . Figure 7 illustrates the correlation between our classification scheme and that of de Sigoyer et al. (2004).

### ***D<sub>1</sub> Structures and Fabrics***

Structures and fabrics developed during the earliest phase of deformation in the Tso Moriri culmination ( $D_1$ ) are extremely rare and their geometry has been obscured by subsequent deformation. Like de Sigoyer et al. (2004), we noted the existence of a relict planar fabric that predates the dominant schistosity and gneissosity in the infrastructure. It is only found in the Puga Gneiss Complex, where  $D_1$  structure is identified as a foliation deformed by later  $F_2$  folds. de Sigoyer et al. (2004) also report steep, tight to isoclinal folds of centimeter scale with a subvertical axial planar cleavage within the orthogneiss, they assigned to the earliest phase of deformation ( $D_A$ ). Based on the geometry of these folds, they concluded that  $D_A$  involved subhorizontal crustal shortening.  $D_A$  of de Sigoyer et al. (2004) is equivalent to the first deformation phase ( $D_1$ ) in our classification scheme. We also follow those authors in interpreting this deformational event as synchronous with the  $M_1$  ultrahigh-pressure metamorphic event.

### ***D<sub>2</sub> Structures and Fabrics***

The dominant planar fabrics in the Puga Gneiss Complex are assigned to  $D_2$ . These mylonitic foliations ( $S_2$ ) have transposed earlier  $S_1$  fabrics, and were later folded

into the broad, doubly-plunging antiform that defines the Tso Morari dome.  $S_2$  is defined by the preferred alignment of mica grains as well as by a gneissic compositional layering. Quartz was dynamically recrystallized, forming up to 2 cm-long ribbons pinned by micaceous layers and displaying a strong lattice-preferred orientation. Up to meter-scale isoclinal folds ( $F_2$ ) with axial surfaces parallel to the schistosity are common throughout the Puga Gneiss Complex (Fig. 2b). Stretching lineations ( $L_2$ ) on  $S_2$  planes are defined by elongate quartz and feldspar grains and consistently plunge very shallowly with a mean orientation of  $10 \rightarrow 330$ . While the mafic eclogite lenses within the orthogneiss are generally massive, some boudins display  $S_2$  fabric that postdates porphyroblasts of  $M_1$  garnet and omphacite but is defined by layers of secondary ( $M_2$ ) clinopyroxene and garnet. In one location, the shape-preferred orientation of  $M_2$  phengite, amphibole and clinopyroxene defines a subhorizontal  $L_2$  lineation. Based on such observations, we regard the  $M_1$  metamorphic assemblage in the mafic boudins of the Puga Gneiss Complex as prekinematic and the  $M_2$  assemblage as pre- to synkinematic with respect to  $D_2$  fabrics.

In the Zoboshisha Unit, the dominant fabric is a schistosity that dips gently away from the core of the dome, and lies parallel to the  $S_2$  foliation in the Puga Gneiss Complex. This schistosity is well-developed everywhere the Zoboshisha Unit is found; however, it has been significantly disturbed and rotated by the Ribil-Zildat normal fault near Sumdho Village. The schistosity is deflected around 2-5 mm euhedral garnet, indicating that garnet growth was pre- or synkinematic. Weak  $L_2$  lineations are only observed near Tso Kar where they are defined by the elongation of micaceous aggregates and quartz ribbons. The mean orientation of  $L_2$  in the Zoboshisha Unit ( $06 \rightarrow 099$ ) is

indistinguishable from that of  $L_2$  lineations in the adjacent Puga Gneiss Complex (09 → 290). Based on these geometric similarities, we conclude that  $D_2$  affected both tectonostratigraphic units (Fig. 4).

### *The Karla Detachment ( $D_2$ )*

The contact between the Puga Gneiss Complex and the Zoboshisha Unit typically dips gently (20-30°) away from the core of the dome, but is both folded and faulted by younger structures. In most areas, it is distinguished by a change in the color and resistance of outcrops of the two units (Fig. 2c) but the contact itself does not crop out well. The best exposures are on the north and south sides of Puga Valley, upstream from the village of Sumdho. On the south side of the Puga Valley, 3-5 m cliffs of Puga orthogneiss are capped by garnetiferous calc-schist of the Zoboshisha Unit. The same relationship appears again on the north side of the valley but is overturned in a younger ( $D_4$ ), rotated fault block. In each location, the contact is parallel to  $S_2$  in both the Puga Gneiss and the Zoboshisha Units. Beyond the detailed mapping areas, the trace of the contact is easily followed on Landsat 7 imagery.

Steck et al. (1998) regarded this surface as a transposed Ordovician intrusive contact, but the mismatch in metamorphic grade across it leads us to reinterpret it as a ductile shear zone that placed lower-pressure Zoboshisha rocks over the ultrahigh-pressure Puga Gneiss Complex. Its geometry suggest normal-sense movement on the structure and we thus refer to it as the Karla Detachment. We regard the pervasive  $L_2$  lineation in the Puga Gneiss Complex – as well as the less well-developed  $L_2$  lineation in the Zoboshisha Unit – as having formed during slip on the Karla Detachment. This

lineation is also developed in dynamically recrystallized clinopyroxene in some mafic boudins within the Puga Gneiss Complex, suggesting that the fabric developed under eclogite to upper-amphibolite conditions. Due to either a component of coaxial strain, or perhaps to a large degree of rotation as the result of intense non-coaxial strain, these fabrics are remarkably symmetric, making shear-sense determination difficult.

In general, we believe that our  $D_2$  deformational phase correlates with the  $D_B$  deformational phase of de Sigoyer et al. (2004) except for one notable exception. Those authors assigned a  $D_B$  age to NE-trending lineations found in the infrastructure near the infrastructure-suprastructure contact. We believe instead that these lineations are younger and related to the  $D_4$  deformational event.

### ***D<sub>3</sub> Structures and Fabrics***

The  $D_3$  event is, in essence, a continuation of the  $D_2$  event. Structurally above the Zoboshisha Unit lies the Taglang La Formation. The contact between the two units is not exposed in the field, though it is clearly seen in Landsat 7 imagery and from a distance as the base of a package of red-weathering, Fe-rich carbonate which forms the snow-capped peaks east of Thupse Village (Fig. 2d). As was the case for the contact between the Puga Gneiss Complex and the Zoboshisha Unit, the metamorphic discontinuity between high pressure footwall rocks and upper greenschist facies hanging wall rocks forces us to interpret the contact as a fault. We refer to this structure as the Thupse Detachment. The trace of this structure across topography shows that it dips shallowly to the NE, roughly parallel to the Karla Detachment below it. Furthermore, weak stretching lineations and schistosity in the overlying Taglang La Formation are parallel to both the fabrics in the

Zoboshisha Unit and the Thupse Detachment itself. However, along the southwest side of the Puga Gneiss Complex, the orthogneiss is in contact with the Taglang La Formation, which requires that underneath the lake sediments that stretch NNE of Tso Kar, the Zoboshisha Unit is cut out by the fault overlying it (Fig. 4).

The fault can be traced around the nose of the dome to the south, where it continues to put the Puga Gneiss Complex in contact with the Taglang La Formation. Roughly 12 km NW of Karzok Village, the fault cuts up through the section, placing the Lamayuru Formation in the hanging wall against the Puga Gneiss Complex. Here the Thupse Detachment dips more steeply ( $\sim 40^\circ$  SW), an attitude which is mimicked by both the schistosity in the footwall and compositional layering in the hanging wall. de Sigoyer et al. (2004) mapped a structure they refer to as the Karzok shear zone along the southwestern margin of the Puga Gneiss Complex. They described the structure as a 5 km-wide, south dipping ductile shear zone that records top-to-the-southwest shear criteria. We found that the top of the proposed shear zone, or the lower contact with the Karzok complex, did not separate tectonic units with significantly disparate metamorphic histories. Rather, we prefer the earlier interpretation of Steck et al. (1998) that this contact represents an older reverse fault, forming the base of the Mata Nappe. Furthermore, below this structure, we found sedimentary rocks displaying minimal deformation and very low metamorphic grade, and not a 5 km-wide mylonitic shear zone. These sediments correspond to the Lamayuru formation, and are separated from the underlying Puga Gneiss Complex by the Thupse Detachment, which is located approximately at the base of the proposed Karzok shear zone of de Sigoyer et al. (2004).



#### ***D<sub>4</sub> Structures and Fabrics***

The fourth deformational event ( $D_4$ ) is marked by the development of a NE-trending stretching lineation ( $L_4$ ) within the Zoboshisha Unit near Sumdho Village (Fig. 2), as well as in the Puga Gneiss Complex near its southwestern margin (Fig. 1). Near Sumdho Village, a few outcrops of garnetiferous schist of the Zoboshisha Unit display an intense crenulation on a scale of 1-3 cm which is absent from the coarser-grained orthogneiss. This crenulation is defined by kinks in mica-rich  $S_2$  bands, and recrystallized ribbon quartz follows the crenulation.  $D_4$  resulted in the formation of no easily discernable, penetrative planar fabric; lineations are instead developed parallel to  $S_2$  planes. However, we observed a very weak composite fabric in a few samples from both the Zoboshisha Unit and the Puga Gneiss Complex which suggest top-to-the-northeast shearing parallel to  $L_4$ , though considerable ambiguity remains in this shear-sense indication. Contrasting shear-sense interpretations of Steck et al. (1998) and de Sigoyer et al. (2004) attest to the uncertainty that persists in this fabric. The intensity of  $L_4$  in the Zoboshisha Unit along only the margin of the infrastructure implies deformation in the shallow crust, near the brittle-ductile transition, in the footwall of the Ribil-Zildat Fault.

The northeastern limb of the Tso Morari culmination is cut by a brittle, high-angle structure. We refer to this structure as the Ribil-Zildat normal fault, being a synthesis of previous names given to the structure by other authors (Zildat Fault of Thakur and Viridi, 1979 and the Ribil Fault of Steck et al., 1997). In the Ribil Valley, this spectacular fault (Fig. 5) juxtaposes greenschist-lower amphibolite facies Sumdho Complex against eclogite facies infrastructure rocks of the Puga Gneiss Complex. However, in the Sumdho

Valley, the footwall of the Ribil-Zildat Fault contains rocks from the Zoboshisha Unit of  $M_2$  conditions, indicating that the metamorphic discontinuity across the structure is not as great as is suggested farther to the south. Along most of its trace, the Ribil-Zildat fault strikes  $\sim 325-145^\circ$  and dips  $\sim 60^\circ$  NE, truncating  $D_2$  and  $D_3$  footwall fabrics (Fig. 3) as well as the Thupse and Karla Detachments. Near Sumdho Village, in the Zildat Valley, the fault expands to a brittle fault zone that is roughly 0.5 km wide. Within this zone, large, fault-bounded blocks of the Puga Gneiss Complex, Zoboshisha Unit, and Sumdho Complex are brecciated, rotated and mantled by gouge.

It has been suggested by other authors (Thakur, 1983; Steck et al., 1998; de Sigoyer et al., 2004) that this fault alone accommodated exhumation of the ultra-high pressure rocks from great depth. However, field observations show that the fault is a brittle structure, active at relatively shallow depth, and is not likely responsible for the  $>90$  km of displacement necessary for exhuming the ultra-high pressure terrain.

Alternately, we suggest that the Ribil-Zildat Fault represents the most recently active, brittle expression of deformation related to the doming process in the area. We believe that doming occurred in the Tso Morari area in a method similar to many of the core complexes of the United States Cordillera. The rolling-hinge model (Axen et al., 1995; Axen and Bartley, 1997) provides a mechanism for the fault geometries observed in the Tso Morari dome.  $L_4$  records elongation in the direction of motion on the Ribil-Zildat fault, while crenulations in the Zoboshisha Unit may result from a phase of shortening as the flexural hinge passed through (Manning and Bartley, 1994). The oldest zircon fission track dates reported by Schlup et al. (2003) are near Tso Morari, and they become progressively younger towards the northeast, with the youngest reported age of  $7.5 \pm 1.5$

Ma a few hundred meters south of the Ribil-Zildat Fault. Such a trend in cooling ages is consistent with the rolling-hinge model, in which doming occurs as an isostatic response to unroofing of the footwall of a high-angle normal fault, and migrates towards the fault as unroofing continues.

### *D<sub>5</sub> Structures and Fabrics*

The most recent deformation in the infrastructure has resulted in an en echelon series of NNE-striking normal faults that collectively define the Tso Morari graben (Fig. 1) and small rift systems. Along the western shore of the Tso Morari itself, the most spectacular of the recent normal faults dips steeply west, exposing footwall orthogneiss. To the north of the Tso Morari, Kiagar Tso occupies a similar position in a smaller graben. Partially degraded fault scarps are visible in the abandoned lake sediments surrounding Kiagar Tso. Both to the north and south of Kiagar Tso, numerous NNE-SSW trending breaks can be traced in the topography and satellite imagery and are interpreted as young, high-angle normal faults. In an isolated, structurally disrupted block north of Tso Kar, the Thupse detachment is overturned, and outcrops of orthogneiss from the Puga Gneiss Complex lie above the characteristic red-weather carbonate of the Taglang La Formation. While the structures responsible for this disruption are hidden by later lacustrine sedimentation, we interpret it as D<sub>5</sub> extensional deformation related to the formation of the Tso Kar basin.

Other modern valleys in the dome appear to be of extensional origin and D<sub>5</sub> fault-controlled. For example, the Puga Valley – which exhibits numerous hot springs and native sulfur deposits – is an asymmetric graben bound to the north by a high-angle,

NNE-striking normal fault and to the south by moderately to shallowly northward-dipping normal fault system. The overall geometry of the valley is strikingly similar to the Death Valley graben of the southwestern United States, replete with well-formed turtleback surfaces on the northward-dipping fault system (cf., Drewes, 1959; Hayman et al., 2003).

## **Structural Evolution of the Suprastructure**

Although our mapping concentrated on the Tso Morari infrastructure, we also examined fabrics in the adjacent suprastructural units to evaluate the relative timing of deformational events in the infrastructure and the juxtaposition of the infrastructure and the suprastructure. The most critical observations are that: 1) fabrics in the Taglang La Formation overlying the Thupse Detachment are parallel to those in the Zoboshisha Unit and Puga Gneiss Complex below; and 2) ductile fabrics in the Sumdho Complex are distinct from those in the footwall of the Ribil-Zildat normal fault.

In the Taglang La Formation above Thupse Village, primary compositional layering is preserved throughout, while weak schistosity ( $S_3$ ) in calc-schist and meta-rhyolite horizons have developed parallel to the compositional layering. Foliation in the Taglang La Formation is parallel to the schistosity in the Zoboshisha Unit, with mean poles to foliation planes of  $61 \rightarrow 195$  and  $68 \rightarrow 189$ , respectively. Weak stretching lineations developed in more micaceous members of the Taglang La Formation are horizontal and trend ESE-WNW, again similar to  $L_3$  lineations in the Zoboshisha Unit and the inferred motion on the Thupse Detachment. These similarities suggest that the Zoboshisha Unit and Taglang La Formation were juxtaposed during the  $D_3$  event.

In the Sumdho Complex, primary compositional layering in slates and carbonates is parallel to schistosity developed in calc-schist and meta-volcanic horizons. In the immediate hanging wall of the Ribil-Zildat normal fault, which itself dips  $60^\circ$  with a strike of  $325^\circ$ , this foliation averages  $\sim 310/50$  NE as opposed to the  $285/13$  N orientation of the  $S_2$  fabric in the footwall Zoboshisha Unit. This structural discontinuity suggests that the Ribil-Zildat normal fault was responsible for brittle deformation and rotation of pre-existing foliations near the surface rather than the formation of ductile fabrics at depth.

### **Exhumation of Ultrahigh-Pressure Rocks in the Tso Morari Dome**

de Sigoyer et al. (2004) presented an evolutionary model for the Tso Morari culmination in which ultrahigh-pressure rocks were exhumed largely in two phases. The first event ( $D_A$ ) was responsible for exhumation from  $M_1$  ultrahigh-pressure conditions to  $M_2$  high-pressure conditions, and was attributed to corner flow in an accretionary prism setting, as described by Platt (1986) and Allemand and Lardeau (1997). The second ( $D_B$ ) was attributed to tectonic denudation from  $M_2$  to  $M_3$  pressures by progressive slip on the Ribil-Zildat normal fault. In the model, mylonitic fabrics at the margin of the infrastructure are interpreted as deep-level fabrics developed on the Ribil-Zildat structure that were progressively overprinted by  $D_C$  brittle fabrics during exhumation, a common characteristic of detachments in the metamorphic core complexes of the North American Cordillera (cf., Davis et al., 1988).

Our structural mapping and analysis of deformational fabrics suggests a somewhat different exhumation history that features progressive exhumation by slip on a

nested system of rooted detachments (Fig. 8). We do not favor the corner flow model for early exhumation of the Puga Gneiss Complex for a variety of reasons. Corner flow models generally do not explain the exhumation of large, coherent tracts of eclogites such as that found at Tso Morari. They are more successful at explaining the exhumation of small, disaggregated blocks of eclogite entrained in a low viscosity ( $<10^7 \text{ Pa}\cdot\text{s}^{-1}$ ) matrix (Cloos and Shreve, 1988). de Sigoyer et al. (2004) point to the existence of serpentinites along the Ribil-Zildat Fault zone as relicts of a low-viscosity matrix that might have enabled corner-flow exhumation of the Puga Gneiss Complex. However, our mapping reveals that serpentinites along the Ribil Fault zone are simply tectonic slivers of the overlying Sumdho Complex within the Ribil-Zildat fault zone, and do not form a matrix for the ultrahigh-pressure part of the infrastructure.

Instead, we believe that the bulk of exhumation from ultrahigh-pressure conditions is better explained by slip on the D<sub>2</sub> Karla Detachment, juxtaposing the Puga Gneiss Complex with the Zoboshisha Unit at high pressure conditions, and continuing exhumation to M<sub>2</sub> amphibolite facies conditions by slip on the D<sub>3</sub> Thupse Detachment. The fault geometries and metamorphic discontinuities are consistent with a model in which these structures accommodated southward extrusion of the Puga Gneiss Complex from beneath the Indus-Tsangpo suture in a manner similar to that envisioned by Chemenda et al. (1996). However, the exhumation path was more complicated than that envisioned by the 2-D analog models of Chemenda and coworkers, since a significant component of the transport occurred in an arc-parallel direction based on the orientation of L<sub>2</sub> lineations. Such motion could be related to early obliquity of collision between the Indian and Asian plates resulting in a strain field that may drive some arc-parallel motion.

Alternatively, such motion may be the result of lateral variability in the density structure of the orogen, resulting in buoyant forces driving the rising Puga Gneiss Complex laterally.

In the absence of geochronologic data from minerals grown synkinematically, indirect age constraints on the deformational events come from the chronology of the three main metamorphic events outlined above. Similarly, without piercing points across any of the major structures, metamorphic discontinuities provide the only means to gauge the “tectonostratigraphic throw” incurred during each deformational event. D<sub>1</sub> occurred under peak metamorphic conditions, at >90 km depth, approximately 45-55 M.y. ago (de Sigoyer et al., 2000; Leech et al., in press) (Fig. 6). The D<sub>2</sub> event brought the Puga Gneiss Complex to high pressure conditions where it was juxtaposed with the Zoboshisha formation. No quantitative P-T estimates or geochronologic constraints are available for this event. Further exhumation occurred on the Thupse Detachment (D<sub>3</sub>) bringing the combined Puga Gneiss Complex and Zoboshisha Unit to amphibolite facies conditions at  $9 \pm 3$  kbar or roughly 30 km depth. This M<sub>2</sub> event occurred at 41-48 Ma (de Sigoyer et al., 1997; Guillot et al., 1997), suggesting that the combined Karla and Thupse Detachments accommodated exceptionally rapid exhumation with a minimum throw of 60 km. Since the L<sub>2</sub> fabric associated with this deformation is strongly oblique to the structures themselves, absolute displacement on these structures may be much greater still. The D<sub>4</sub> event brought the Tso Morari culmination to M<sub>3</sub> conditions very near the surface by 29-31 Ma, and continuing through ~7 Ma (de Sigoyer et al., 2000; Schlup et al., 2003). These final ~30 km of denudation were accomplished by a combination of isostatic equilibration as a result of the tectonic denudation that occurred on the Ribil-

Zildat normal fault and erosive removal of domed overburden. D<sub>5</sub> extension perhaps has assisted in the final denudation of the Tso Morari culmination, has clearly been recently active, and may continue at present.

## **Relation to Other North Himalayan Gneiss Domes**

The Tso Morari culmination shares a number of structural similarities with the series of north Himalayan gneiss domes to the east (Hodges, 2000). However, previously studied domes (Chen et al., 1990; Guillot et al., 1998; Lee et al., 2000; Murphy et al., 2002; Lee et al., 2004; Murphy and Copeland, in press?) have exhumational histories featuring substantial tectonic denudation in Miocene time. In contrast, thermochronologic data for Tso Morari suggest exhumation in Oligocene time as suggested above.

Furthermore, many of the North Himalayan gneiss domes record a significant Miocene thermal event, which resulted in new magmatism and abundant migmatite in some terrains (Scharer et al., 1986; Harrison et al., 1999; Lee et al., 2000). Such a record is absent from the Tso Morari culmination.

Field relations and geochronological data suggest that doming of the Tso Morari culmination occurred by a simple, rolling-hinge mechanism, rather than through a series of complex compressional and extensional events as described in many of the Himalayan Gneiss Domes further east. In the core-complexes of the North American Cordillera, exhumation is generally the result of tectonic denudation on a single detachment surface, showing unidirectional kinematics across the dome. In rolling hinge models, this detachment is observed as an active, steeply dipping ramp that is progressively rotated as an antiformal hinge moves through the footwall, and eventually abandoned, leaving an inactive, low-angle fault surface behind (Spencer, 1984; Buck, 1988). In the Tso Morari



culmination, the active fault is present as the brittle, high-angle Ribil-Zildat normal fault, while in our study area, the remnant low-angle fault surface has been eroded away. Exhumation progressed across the dome from southwest to northeast, as indicated by the fission track data of Schlup et al. (2003). Kinematic indicators are difficult to find, because of the lack of well-developed planar fabrics during the D<sub>4</sub> event. However, where shear-sense criteria could be observed, we consistently observed top to the northeast motion across the dome. Continued study should include structural mapping further south in an attempt to identify the abandoned segment of the major detachment responsible for the doming, as well as detailed studies of quartz lattice-preferred orientations within the Puga Gneiss Complex in order to try to accurately constrain the kinematics of the D<sub>4</sub> event.

## **Discussion and Conclusions**

Deformational structures in the Tso Morari culmination suggest a polyphase history of extensional deformation. Subsequent to peak metamorphism, the Puga Gneiss Complex was exhumed from ultrahigh-pressure eclogite facies along the Karla Detachment and juxtaposed with the Zoboshisha Unit at amphibolite facies. Rapid exhumation during this deformational event was likely driven by density contrasts between the relatively buoyant Puga Gneiss Complex and the mantle wedge beneath the Eurasian continent under which it was subducted. This exhumation involved a significant amount of arc-parallel motion, perhaps a result of lateral heterogeneity in the density structure through which the material was rising. A second phase of extrusion occurred on the Thupse Detachment, which brought the combined Zoboshisha Unit and Puga Gneiss

Complex to upper greenschist facies and into contact with the Taglang La Formation. This motion likely represents the last stage of buoyant rise, as large density contrasts no longer existed between the Tso Morari infrastructure and its surroundings once it reached upper crustal depths.

The final stages of exhumation of the infrastructure were accommodated by structures responsible for the classic metamorphic core complex morphology of the Tso Morari dome. We interpret the dome, bounded to the north by the Ribil-Zildat fault, in terms of a rolling-hinge model (Spencer, 1984; Wernicke, 1985; Buck, 1988; Axen et al., 1995; Axen and Bartley, 1997). Contrary to studies of other Himalayan Gneiss Domes, the domal structure of the Tso Morari culmination was driven by relatively simple mechanisms similar to those observed in metamorphic core complexes of the North American Cordillera.

Finally, very young and potentially active N-S striking normal faults define a large graben structure in the Puga Gneiss Complex, in which Tso Morari and Kiagar Tso are situated. These recent structures, as well as the high heat flow implied by hydrothermal activity in the Puga Valley, imply that extension has occurred in the Tso Morari area, at least sporadically, over much of Tertiary time despite a setting within one of the most spectacular collisional orogens on Earth.

## References Cited

- Allemand, P., and Lardeaux, J.-M., 1997, Strain partitioning and metamorphism in a deformable orogenic wedge; application to the Alpine belt  
Thermal and mechanical interactions in deep-seated rocks: Symposium on Thermal and mechanical interactions in deep-seated rocks, v. 280, p. 157-169.
- Armstrong, R.L., 1982, Cordilleran metamorphic core complexes; from Arizona to southern Canada: Annual Review of Earth and Planetary Sciences, v. 10, p. 129-154.
- Axen, G.J., and Bartley, J.M., 1997, Field tests of rolling hinges; existence, mechanical types, and implications for extensional tectonics: Journal of Geophysical Research, B, Solid Earth and Planets, v. 102, p. 20,515-20,537.
- Axen, G.J., Bartley, J.M., and Selverstone, J., 1995, Structural expression of a rolling hinge in the footwall of the Brenner Line normal fault, Eastern Alps: Tectonics, v. 14, p. 1380-1392.
- Beaumont, C., Jamieson, R.A., Nguyen, M.H., and Lee, B., 2001, Himalayan tectonics explained by extrusion of a low-viscosity crustal channel coupled to focused surface denudation: Nature (London), v. 414, p. 738-742.
- Berthelsen, A., 1953, On the geology of the Rupshu District, N. W. Himalaya; a contribution to the problem of the central gneisses: Bulletin of the Geological Society of Denmark = Meddelelser fra Dansk Geologisk Forening, v. 12, p. 350-414.
- Buck, W.R., 1988, Flexural Rotation of Normal Faults: Tectonics, v. 7, p. 959-973.
- Burchfiel, B.C., Zhiliang, C., Hodges, K.V., Yuping, L., Royden, L.H., Changrong, D., and Jiene, X., 1992, The South Tibetan detachment system, Himalayan Orogen; extension contemporaneous with and parallel to shortening in a collisional mountain belt: Special Paper - Geological Society of America, v. 269, p. 41.
- Chemenda, A., Mattauer, M., and Bokun, A.N., 1996, Continental subduction and a mechanism for exhumation of high-pressure metamorphic rocks: new modeling and field data from Oman: Earth and Planetary Science Letters, v. 143, p. 173-182.
- Chen, Z., Liu, Y., Hodges, K.V., Burchfiel, B.C., Royden, L.H., and Deng, C., 1990, The Kangmar Dome; a metamorphic core complex in southern Xizang (Tibet): Science, v. 250, p. 1552-1556.
- Cloos, M., and Shreve, R.L., 1988, Subduction-channel model of prism accretion, mélangé formation, sediment subduction, and subduction erosion at convergent plate margins; Part II, Implications and discussion: Pure and Applied Geophysics, v. 128, p. 501-545.
- Colchen, M., Mascle, G., and Delaygue, G., 1994, Lithostratigraphy and age of the formations in the Tso Morari dome: Journal of Nepal Geological Society, v. 10, p. 23.
- Coney, P.J., and Reynolds, S.J., 1980, Cordilleran metamorphic core complexes; an overview, *in* Crittenden, M.D., Coney, P.J., and Davis, G.H., eds., Cordilleran Metamorphic Core Complexes, Volume 153: Geological Society of America Memoir: Boulder, Geological Society of America, p. 7-34.
- Davis, G.A., Lister, G.S., Clark, S.P., Jr. (editor), Burchfiel, B.C.e., and Suppe, J.e., 1988, Detachment faulting in continental extension; perspectives from the Southwestern U.S. Cordillera Processes in continental lithospheric deformation: Special Paper - Geological Society of America, v. 218, p. 133-159.
- de Sigoyer, J., 1998, Mécanismes d'exhumation des roches de haute pression basse température, en contexte de convergence continentale (Tso Morari, NW Himalaya) [Ph.D. thesis]: Lyon, France, Univ. Claude Bernard.

- de Sigoyer, J., Chavagnac, V., Blichert-Toft, J., Villa, I.M., Luais, B., Guillot, S., Cosca, M., and Mascle, G., 2000, Dating the Indian continental subduction and collisional thickening in the northwest Himalaya: Multichronology of the Tso Morari eclogites: *Geology*, v. 28, p. 487-490.
- de Sigoyer, J., Guillot, S., and Dick, P., 2004, Exhumation of the ultrahigh-pressure Tso Morari Unit in eastern Ladakh (NW Himalaya); a case study: *Tectonics*, v. 23, p. 18.
- de Sigoyer, J., Guillot, S., Lardeaux, J.M., and Mascle, G., 1997, Glaucophane-bearing eclogites in the Tso Morari dome (eastern Ladakh, NW Himalaya): *European Journal of Mineralogy*, v. 9, p. 1073-1083.
- Drewes, H.D., 1959, Turtleback faults of Death Valley, California; a reinterpretation: *Geological Society of America Bulletin*, v. 70, p. 1497-1508.
- Gaetani, M., and Garzanti, E., 1991, Multicyclic History of the Northern India Continental-Margin (Northwestern Himalaya): *Aapg Bulletin-American Association of Petroleum Geologists*, v. 75, p. 1427-1446.
- Garzanti, E., Baud, A., Mascle, G., and Anonymous, 1987, Sedimentary record of the northward flight of India and its collision with Eurasia (Ladakh Himalaya, India) *Colloque Tethys et Himalaya; Tethys and Himalaya colloquium: Colloque Tethys et Himalaya*, EUG, v. 1, p. 297-312.
- Garzanti, E., and Van Haver, T., 1988, The Indus clastics; forearc basin sedimentation in the Ladakh Himalaya (India): *Sedimentary Geology*, v. 59, p. 237-249.
- Girard, M., and Bussy, F., 1999, Late Pan-African magmatism in the Himalaya: new geochronological and geochemical data from the Ordovician Tso Morari metagranites (Ladakh, NW India): *Schweizerische Mineralogische Und Petrographische Mitteilungen*, v. 79, p. 399-418.
- Guillot, S., deSigoyer, J., Lardeaux, J.M., and Mascle, G., 1997, Eclogitic metasediments from the Tso Morari area (Ladakh, Himalaya): evidence for continental subduction during India-Asia convergence: *Contributions to Mineralogy and Petrology*, v. 128, p. 197-212.
- Guillot, S., Lardeaux, J.M., Mascle, G., and Colchen, M., 1995, A New Record of High-Pressure Metamorphism in the Himalayan Range - the Retrogressed Eclogites of the Tso-Morari Dome (East Ladakh): *Comptes Rendus De L Academie Des Sciences Serie Ii*, v. 320, p. 931-936.
- Guillot, S., Pochat, S., Zakarian, N., and Hodges, K.V., 1998, Metamorphic evolution of the Kangmar dome (Se-Xizang, Tibet): implications for the internal Himalayan zones: *Comptes Rendus De L Academie Des Sciences Serie Ii Fascicule a-Sciences De La Terre Et Des Planetes*, v. 327, p. 577-582.
- Guiraud, M., Powell, R., and Rebay, G., 2001, H<sub>2</sub>O in metamorphism and unexpected behavior in the preservation of metamorphic mineral assemblages: *Journal of Metamorphic Geology*, v. 19, p. 445-454.
- Harrison, T.M., Grove, M., McKeegan, K.D., Coath, C.D., Lovera, O.M., and Le Fort, P., 1999, Origin and episodic emplacement of the Manaslu intrusive complex, Central Himalaya: *Journal of Petrology*, v. 40, p. 3-19.
- Hayman, N.W., Knott, J.R., Cowan, D.S., Nemser, E., and Sarna-Wojcicki, A.M., 2003, Quaternary low-angle slip on detachment faults in Death Valley, California: *Geology (Boulder)*, v. 31, p. 343-346.
- Hodges, K.V., 2000, Tectonics of the Himalaya and southern Tibet from two perspectives: *Geological Society of America Bulletin*, v. 112, p. 324-350.

- Holdaway, M.J., 1971, Stability of andalusite and the aluminum silicate phase diagram: American Journal of Science, v. 271, p. 97-131.
- Holland, T.J.B., 1980, Reaction Albite = Jadeite + Quartz Determined Experimentally in the Range 600-1200-Degrees-C: American Mineralogist, v. 65, p. 129-134.
- Kurz, W., and Fritzsche, N., 2002, The exhumation of eclogite-facies metamorphic rocks - a review of models confronted with examples from the Alps: International Geology Review, v. 44, p. 702-743.
- Lee, J., Hacker, B., and Wang, Y., 2004, Evolution of North Himalayan gneiss domes: structural and metamorphic studies in Mabja Dome, southern Tibet: Journal of Structural Geology, v. 26, p. 2297-2316.
- Lee, J., Hacker, B.R., Dinklage, W.S., Yu, W., Gans, P., Calvert, A., Jinglin, W., Wenji, C., Blythe, A.E., and McClelland, W.C., 2000, Evolution of the Kangmar Dome, southern Tibet; structural, petrologic, and thermochronologic constraints: Tectonics, v. 19, p. 872-895.
- Leech, M.L., Singh, S., Jain, A.K., Klemperer, S.L., and Manickavasagam, R.M., in press, The onset of India-Asia continental collision: Early, steep subduction required by the timing of ultrahigh-pressure metamorphism in the western Himalaya: Earth and Planetary Science Letters.
- Maheo, G., Bertrand, H., Guillot, S., Mascle, G., Pecher, A., Picard, C., and De Sigoyer, J., 2000, Evidence of a Tethyan immature arc within the South Ladakh ophiolites (NW Himalaya, India): Comptes Rendus De L Academie Des Sciences Serie Ii Fascicule a-Sciences De La Terre Et Des Planetes, v. 330, p. 289-295.
- Manning, A.H., and Bartley, J.M., 1994, Post-mylonitic Deformation in the Raft River Metamorphic Core Complex, Northwestern Utah - Evidence of a Rolling Hinge: Tectonics, v. 13, p. 596-612.
- Massonne, H.J., and Schreyer, W., 1989, Stability Field of the High-Pressure Assemblage Talc + Phengite and 2 New Phengite Barometers: European Journal of Mineralogy, v. 1, p. 391-410.
- Mukherjee, B.K., and Sachan, H.K., 2001, Discovery of coesite from Indian Himalaya: A record of ultra-high pressure metamorphism in Indian Continental Crust: Current Science, v. 81, p. 1358-1361.
- Mukherjee, B.K., Sachan, H.K., Ogasawara, Y., Moko, A., and Yoshioka, N., 2003, Carbonate-bearing ultrahigh-pressure rocks from the Tso-Morari region, Ladakh, India: Petrological implications: International Geology Review, v. 45, p. 49-69.
- Murphy, M.A., and Copeland, P., in press?, Transtensional deformation in the central Himalaya and its role in accommodating growth of the Himalayan orogen: Tectonics.
- Murphy, M.A., Yin, A., Kapp, P., Harrison, T.M., Manning, C.E., Ryerson, F.J., Lin, D., and Jinghui, G., 2002, Structural evolution of the Gurla Mandhata detachment system, Southwest Tibet; implications for the eastward extent of the Karakoram fault system: Geological Society of America Bulletin, v. 114, p. 428-447.
- Platt, J.P., 1986, Dynamic of orogenic wedges and the uplift of high-pressure metamorphic rocks: Geological Society of America Bulletin, v. 97, p. 1037-1053.
- Rumble, D., Liou, J.G., and Jahn, B., 2003, Continental crust subduction and ultrahigh pressure metamorphism, in Rudnick, R.L., ed., The Crust, Volume 3: Treatise on Geochemistry, Elsevier.
- Sachan, H.K., 2001, Supra-subduction origin of the Nidar ophiolitic sequence, Indus Suture Zone, Ladakh, India: Evidence from mineral chemistry of upper mantle rocks: Ophiolite, v. 26, p. 23-32.

- Sachan, H.K., Bodnar, R.J., Islam, R., Szabo, C., and Law, R.D., 1999, Exhumation history of eclogites from the Tso-Morari crystalline complex in eastern Ladakh; mineralogical and fluid inclusion constraints: *Journal of the Geological Society of India*, v. 53, p. 181-190.
- Scharer, U., Xu, R.H., and Allegre, C.J., 1986, U-(Th)-Pb Systematics and Ages of Himalayan Leucogranites, South Tibet: *Earth and Planetary Science Letters*, v. 77, p. 35-48.
- Schlup, M., Carter, A., Cosca, M., and Steck, A., 2003, Exhumation history of eastern Ladakh revealed by Ar-40/Ar-39 and fission-track ages: the Indus River-Tso Morari transect, NW Himalaya: *Journal of the Geological Society*, v. 160, p. 385-399.
- Smyth, J.R., and Hatton, C.J., 1977, Coesite-Sanidine Grosspydite from Roberts-Victor Kimberlite: *Earth and Planetary Science Letters*, v. 34, p. 284-290.
- Spencer, J.E., 1984, Role of Tectonic Denudation in Warping and Uplift of Low-Angle Normal Faults: *Geology*, v. 12, p. 95-98.
- Steck, A., Epard, J.L., Vannay, J.C., Hunziker, J., Girard, M., Morard, A., and Robyr, M., 1998, Geological transect across the Tso Morari and Spiti areas: The nappe structures of the Tethys Himalaya: *Eclogae Geologicae Helveticae*, v. 91, p. 103-122.
- Steck, A., 2003, Geology of the NW Indian Himalaya: *Eclogae Geologicae Helveticae*, v. 96, p. 147-U13.
- Stutz, E., 1988, Geologie de la chaine de Nymaling aux confins du Ladakh et du Rupshu (NW-Himalaya, Inde); evolution paleogeographique et tectonique d'un segment de la marge nord-indienne; *Geology of the Nymaling Range within the borders of Ladakh and Rupshu, northwestern Himalayas, India; paleogeographic and tectonic evolution of a section of the northern Indian margin: Memoires de Geologie Lausanne*, v. 3, p. 149.
- Thakur, V.C., 1983, Deformation and metamorphism of the Tso Morari crystalline complex, *in* Thakur, V.C., and Sharma, K.K., eds., *Geology of the Indus Suture Zone of Ladakh: Dehra dun, Wadia Institute of Himalayan Geology*, p. 1-8.
- Thakur, V.C., and Bhat, M.I., 1983, Interpretation of tectonic environment of Nidar ophiolite: A geochemical approach, *in* Thakur, V.C., and Sharma, K.K., eds., *Geology of Indus Suture Zone of Ladakh: Dehra Dun, India, Wadia Institute of Himalayan Geology*, p. 33-40.
- Thakur, V.C., and Viridi, N.S., 1979, Lithostratigraphy, structural framework, deformation and metamorphism of the southeastern region of Ladakh, Kashmir Himalaya, India: *Himalayan Geology*, v. 9, p. 63-78.
- Wei, C.J., and Powell, R., 2004, Calculated phase relations in high-pressure metapelites in the system NKFMAH (Na<sub>2</sub>O-K<sub>2</sub>O-FeO-MgO-Al<sub>2</sub>O<sub>3</sub>-SiO<sub>2</sub>-H<sub>2</sub>O): *Journal of Petrology*, v. 45, p. 183-202.
- Wernicke, B.P., 1985, Uniform-sense normal simple shear of the continental lithosphere: *Canadian Journal of Earth Sciences*, v. 22, p. 108-125.

## Figure Captions

Figure 1) Simplified geologic map of the Tso Morari culmination. Light areas are areas that were easily accessed and mapped in detail. Shaded regions show areas where mapping is based on compilation of previous studies (Thakur and Viridi, 1983; Steck et al., 1997; de Sigoyer et al., 2004; Steck 2003) and photo interpretation from Landsat 7 ETM+ images. These 15m resolution panchromatic images allowed us to trace structures mapped in detail into inaccessible terrain with considerable accuracy. A legend for the map is presented on the following page.

Figure 2) A) Mylonitic Puga Orthogneiss. Outcrop is roughly parallel to  $L_2$  stretching lineation, and perpendicular to  $S_2$  schistosity. Note that augens are often quite symmetric, and that asymmetries displayed by a few porphyroclasts indicate conflicting sense-of-shear. B) Small asymmetric, tight, 10cm-scale folds within the Puga Gneiss Complex. These are  $F_2$  folds, folding  $F_1$  compositional layering.  $S_2$  axial planar schistosity is apparent. C) One of two outcrops of the Karla Detachment. Here, the detachment is part of an overturned block related to later deformation on the Ribil-Zildat fault. Above the contact is light weathering orthogneiss of the Puga Gneiss Complex, and below the contact is the darker weathering, garnetiferous Zoboshisha Unit. The contact is parallel to the  $D_2$  fabrics in both the footwall and the hangingwall. D) Distance shot of the Thupse Detachment. We were unable to find a good outcrop of the fault itself, though the distinction between the footwall Zoboshisha Unit, and the red-weathering carbonates of the Taglang La Formation. are very easy to trace both in the field as well as with Landsat 7 ETM+ imagery.

Figure 3) Geologic map of the Ribil-Zildat fault zone and its interaction with the Karla Detachment. Legend is the same as for figure 1. Stereonets show measurements of the dominant  $S_2$  fabric, as well as  $L_2$  and  $L_4$  stretching lineations in the Puga Gneiss Complex and Zoboshisha Unit, and  $S_3$  fabric in the Sumdho Complex. The Ribil-Zildat fault consists of a number of splays over a zone ~1km wide. Blocks within these splays are rotated and mantled by gouge.  $D_2$  fabrics in the footwall are cut by the Ribil-Zildat fault, as is the Karla Detachment itself.  $L_4$  stretching lineations formed in the Zoboshisha Unit here at relatively shallow depth.

Figure 4) Geologic map of the northern tip of the Puga Gneiss Complex, near Tso Kar. Legend is the same as for figure 1. Stereonets show measurements of the dominant  $S_2$  fabric, as well as  $L_2$  stretching lineations in the Puga Gneiss Complex and Zoboshisha Unit, and  $S_3$  fabric in the overlying Taglang La Formation. In this section the parallelism of the Karla Detachment, the Thupse Detachment, and related  $D_2$  and  $D_3$  fabrics are apparent. The Thupse Detachment cuts the Karla Detachment under the lake sediments north of Thupse Village, and is deformed by later  $D_4$  doming.

Figure 5) Distance photograph of the Ribil-Zildat fault. Visible are the numerous splays of the fault, and the truncation of the much more shallowly dipping Karla Detachment.



Figure 6) PT estimates from metasediments and mafic eclogites from within the Puga Gneiss Complex. Yellow boxes represent the ranges of quantitative PT estimates for each metamorphic event, which were obtained by de Sigoyer et al. (1997), Guillot et al. (1997) and Mukherjee and Sachan (2003) using both classic thermobarometry, and Thermocalc software. Dashed lines are contours of Si concentration in phengitic mica, in the limiting assemblage with talc, kyanite and coesite (Massonne and Schreyer, 1989). The green line represents the contour for Si = 3.63, the maximum concentration observed by Mukherjee and Sachan (2003). Timing of metamorphic events is from de Sigoyer et al. (2000), Leech et al. (in press) and from unpublished preliminary U-Pb dates from eclogitic zircons analyzed at MIT. The coesite/quartz transition is from Smyth and Hatton (1977). The reaction  $Jd + Qtz = Ab$  is from Holland (1980). The aluminum-silicate triple-point is from Holdaway (1971) [55].

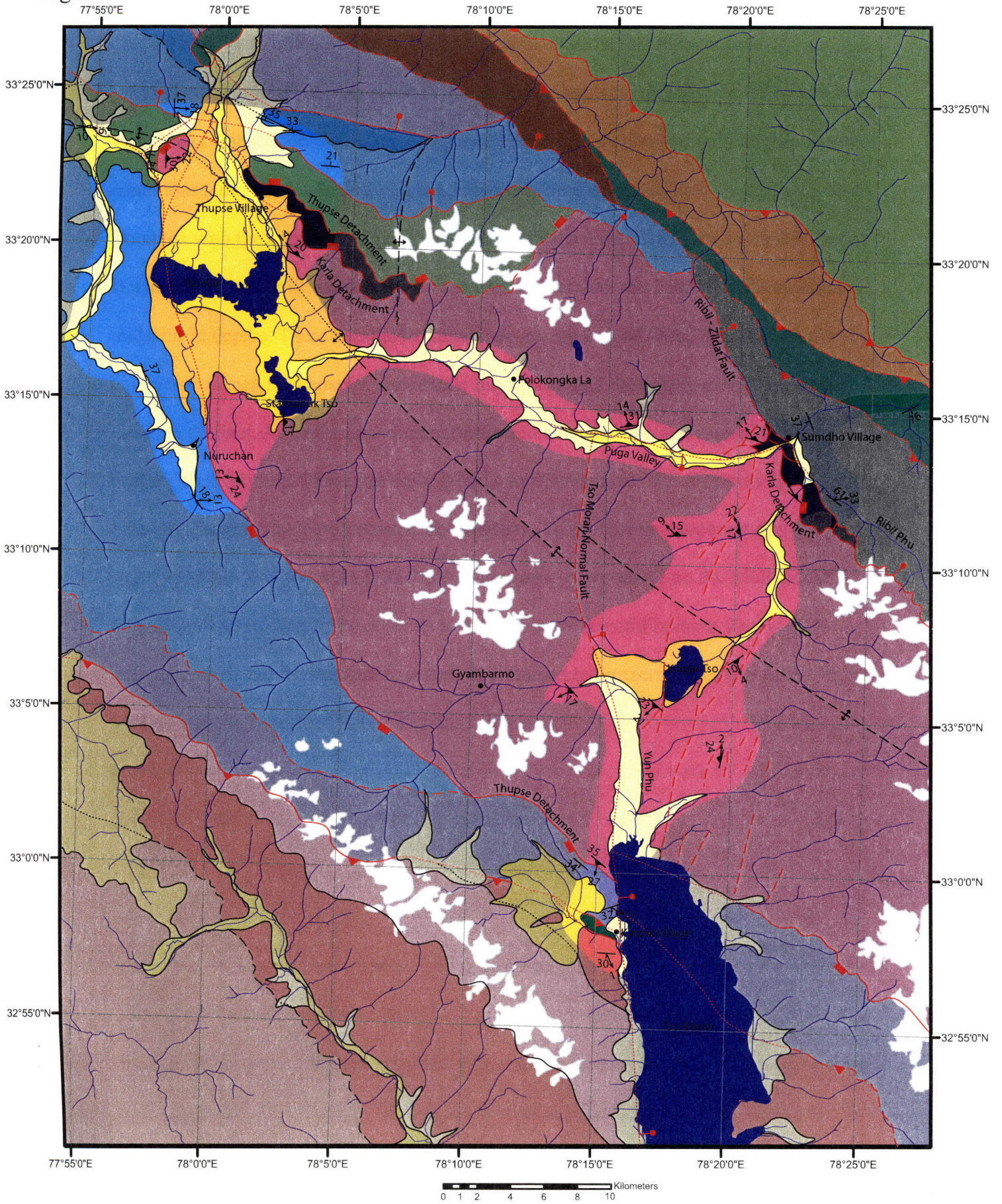
Figure 7) Diagram showing correlation between the deformational events of this study, and those of de Sigoyer et al. (2004). Grey bars indicate which deformational events are recorded in each unit, while colored bars correspond to metamorphic events. Dashed ends to metamorphic bars indicate that the precise onset of metamorphism with respect to the timing of deformational events is unknown.

Figure 8) Evolutionary diagram for the Tso Moriri culmination. Color scheme is the same as that for the geological maps (Fig. 1, 3, 4). Block models on the left portray the general geometry of the Himalayan orogen, and indicate the planes of each of the cross sections to the right. The first three deformational events record extension roughly

parallel to the axis of the orogen, while the final two events record extension perpendicular to it. D<sub>1</sub> records sub-horizontal shortening under eclogite facies conditions in the Puga Gneiss Complex. D<sub>2</sub> records the bulk of exhumation from ultrahigh-pressure conditions along the Karla Detachment, juxtaposing the eclogite-facies Puga Gneiss Complex with the upper-amphibolite grade Zoboshisha Unit. Extension along the Thupse Detachment brought these combined units into contact with the Taglang La Formation at mid-crustal depths. These two deformational events were most likely driven by buoyancy contrasts between the dense, Asian mantle lithosphere and the orthogneiss of the Puga Gneiss Complex. At this point exhumation slowed considerably, and moved into the brittle-ductile regime. Through a rolling-hinge mechanism like that proposed for many core-complexes in the North American Cordillera, D<sub>4</sub> saw the development of the domal structure of the Tso Morari culmination, as progressive unroofing on the Ribil-Zildat normal fault allowed uplift to occur as a result of isostatic equilibration. Recent, N-S striking graben and rift structures, as well as abundant hydrothermal activity in the Puga Valley, attest to continued E-W extension in the area.



Figure 1





# Legend




## Quaternary

-  Wetland Cover
-  Glaciers
-  Alluvial Sediments
-  Alluvial Fans and Landslide deposits
-  Lacustrine Sediments

## Eocene

-  Indus Mollase
-  Undifferentiated Indus Suture Zone Rocks

## Mesozoic

-  Ladakh Batholith
-  Sumdho Complex
-  Nidar Ophiolite and Karzok Complex


## Paleozoic


-  Lamayuru Formation
- Taglang La Formation
-  Meta-Rhyolite Member
  -  Siliciclastic Member
  -  Fe-rich Carbonate Member

-  Zoboshisha Unit

-  Rupshu Granite
-  Puga Gneiss Complex
-  Lilang/Kuling Fm
-  Phe Formation

 Contact, dashed where approximate, dotted where covered

 High Angle Fault, normal sense, dashed where approximate, dotted where covered

 Low angle fault, normal sense, dashed where approximate, dotted where covered

 Reverse sense fault, dashed where approximate, dotted where covered

 Anticline, approximately located

 Orientation of Compositional Layering

 Orientation of primary bedding

 Stretching Lineation

Figure 2

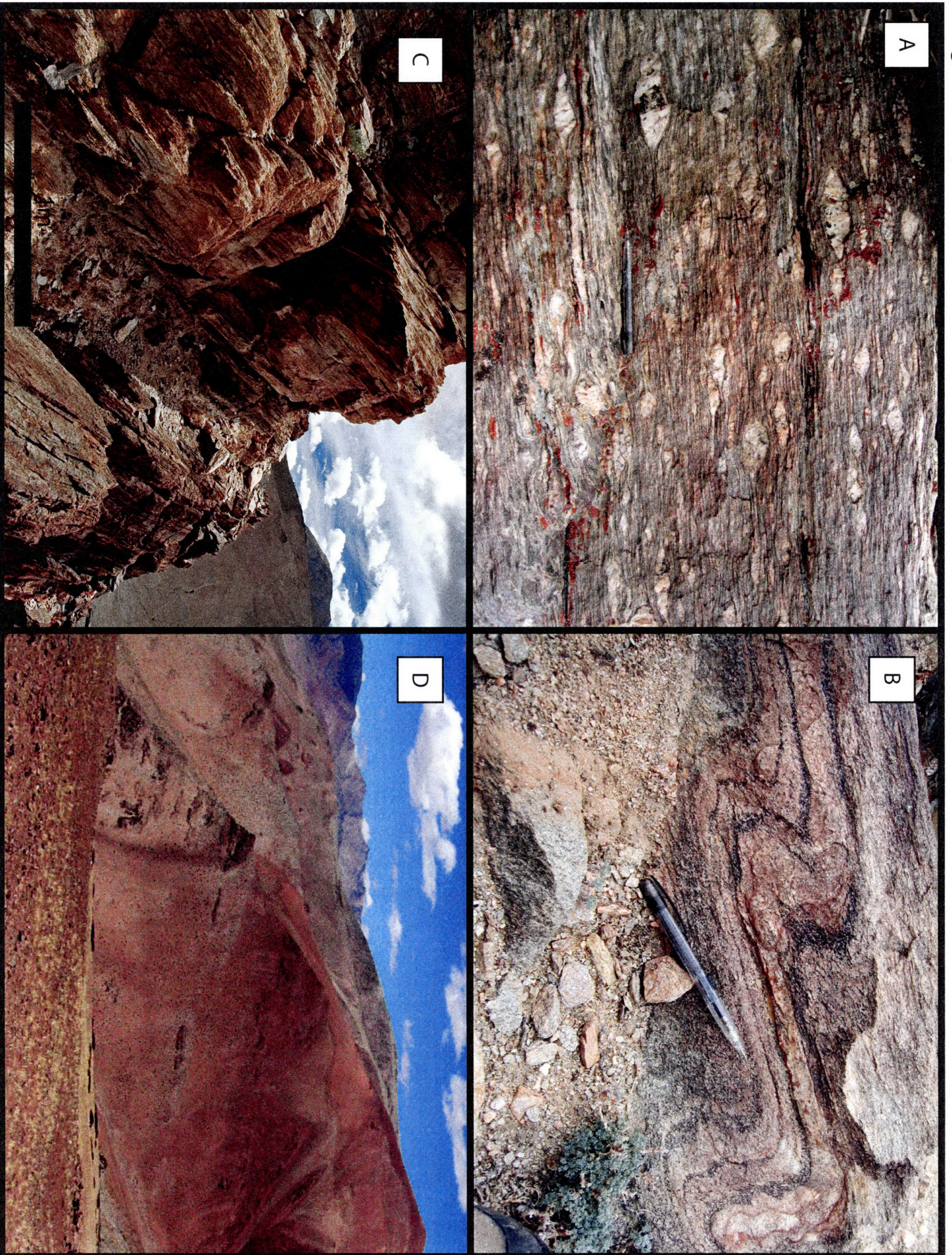


Figure 3

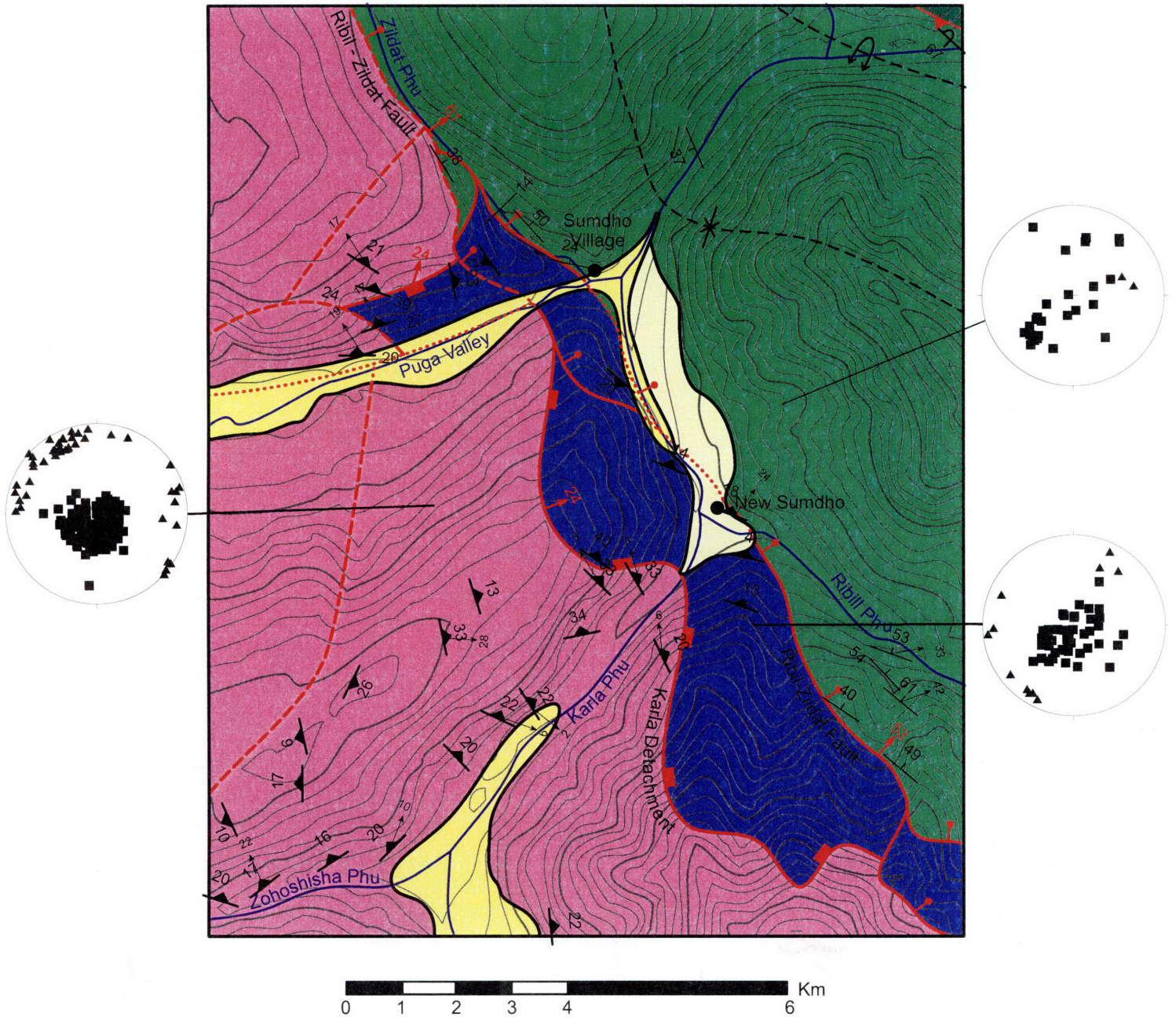


Figure 4

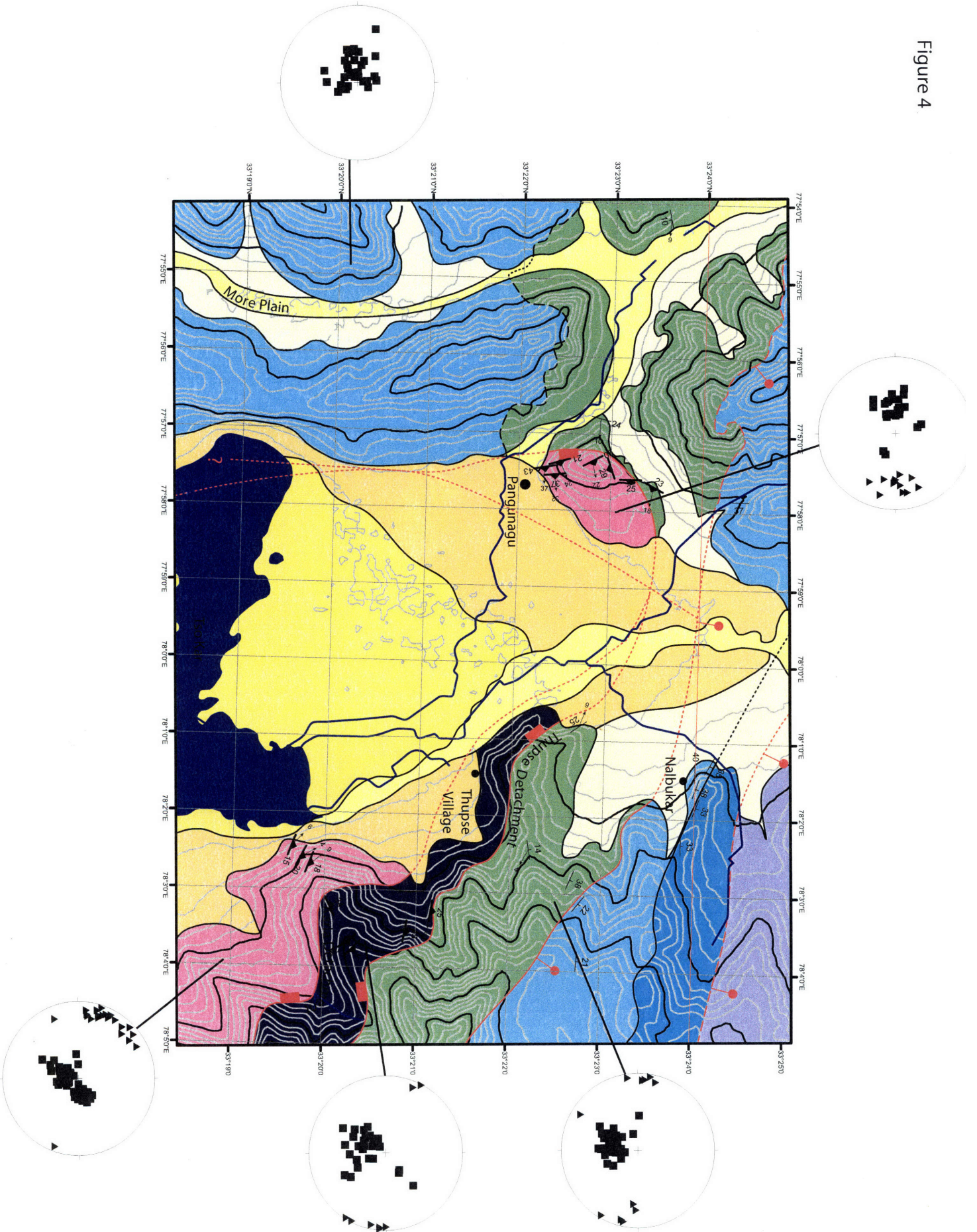




Figure 5

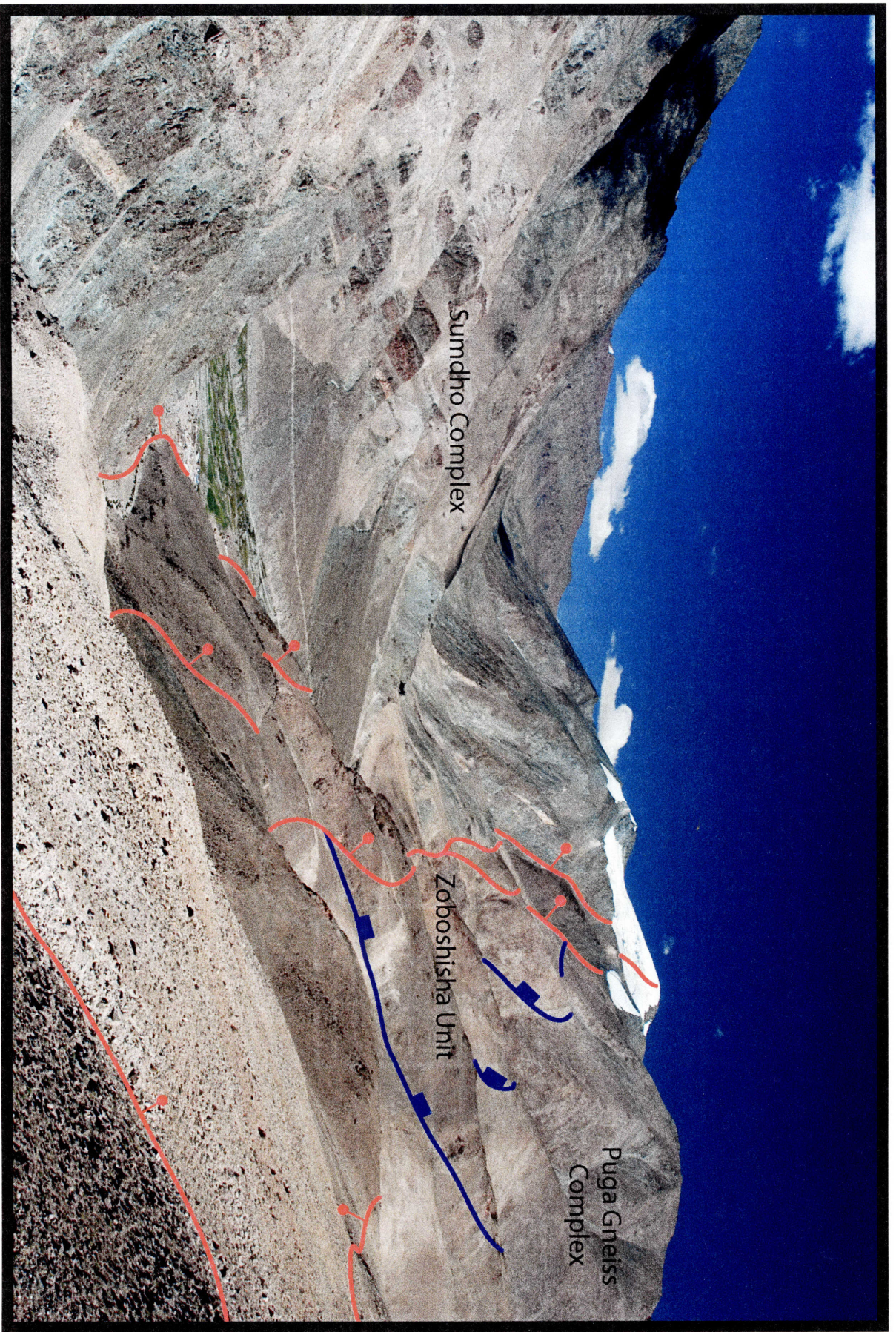


Figure 6

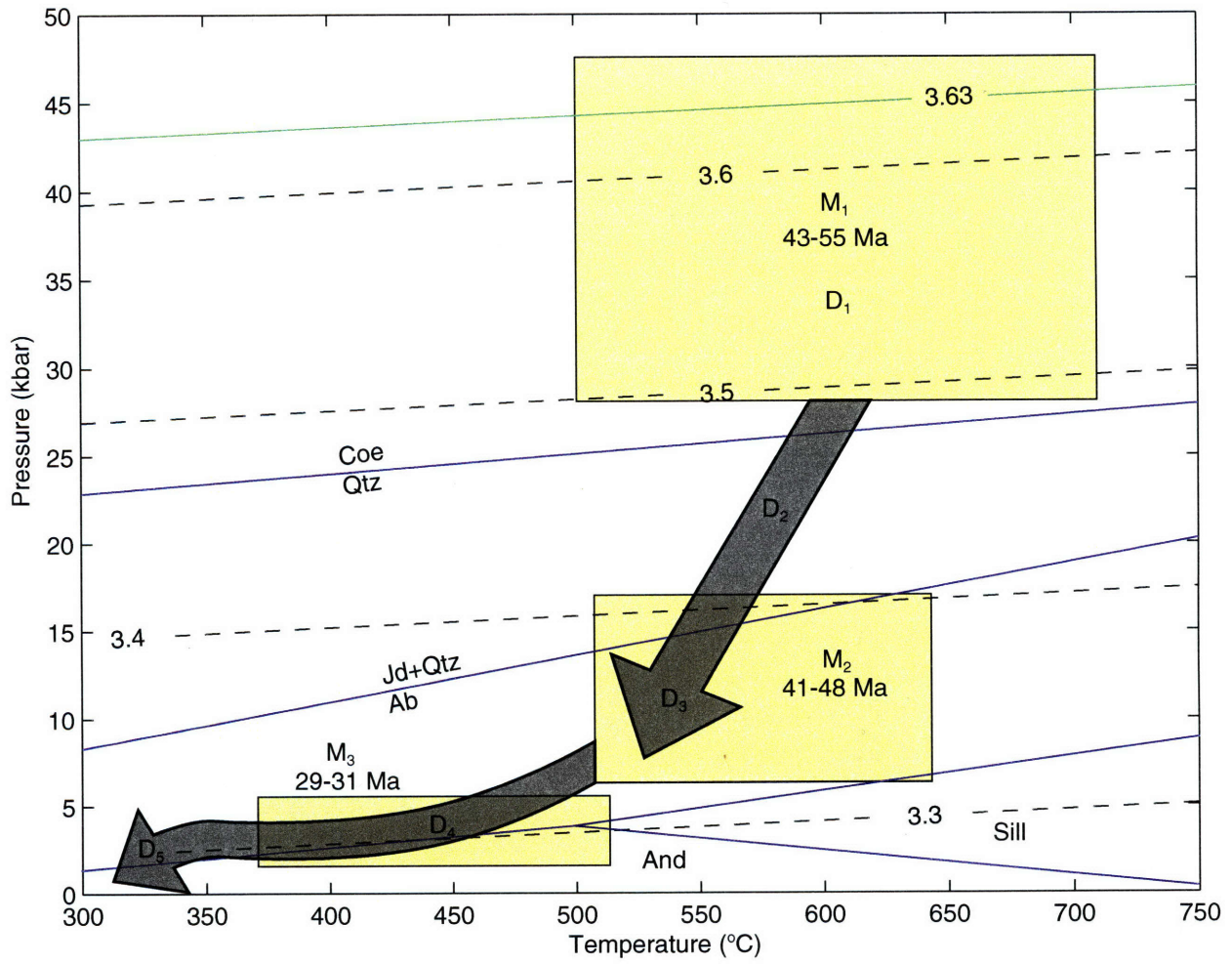


Figure 7

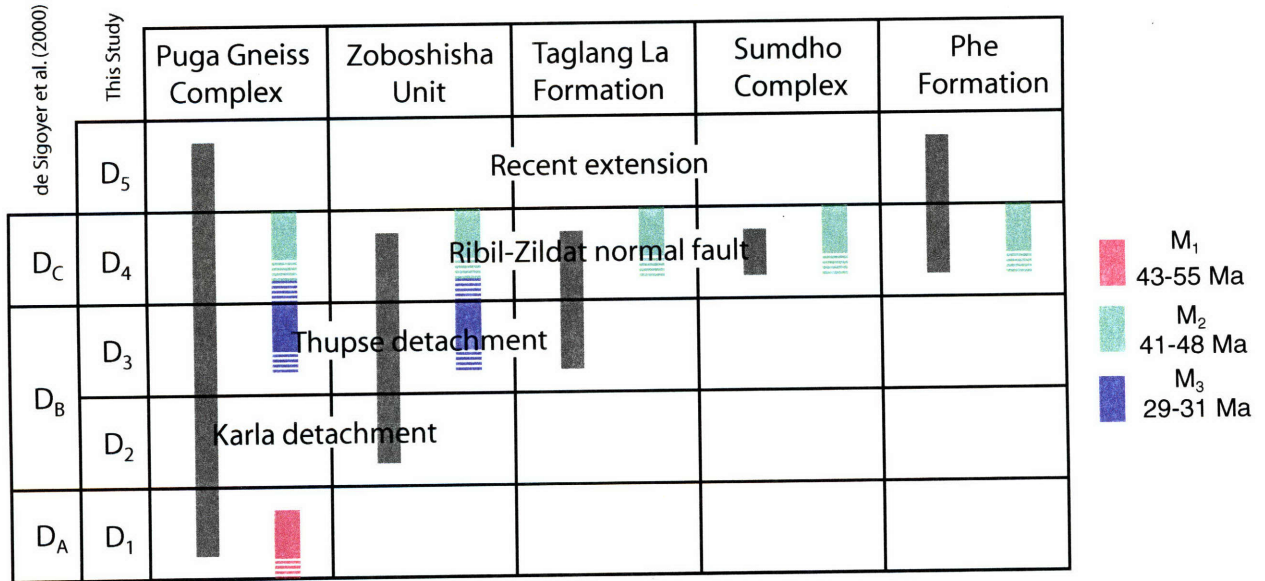


Figure 8

